Capabilities and limitations of pupil-plane filters for superresolution and image enhancement

Brynmor J. Davis, William C. Karl, Anna K. Swan, M. Selim Ünlü

Department of Electrical and Computer Engineering, Boston University, Boston, MA 02215, USA

bryn@bu.edu, wckarl@bu.edu, swan@bu.edu, selim@bu.edu

Bennett B. Goldberg

Department of Physics and Department of Electrical and Computer Engineering, Boston University, Boston, MA 02215, USA

goldberg@bu.edu

Abstract: The use of pupil-plane filters in microscopes has been proposed as a method of producing superresolution. Here it is shown that pupil-plane filters cannot increase the support of the transfer function for a large class of optical systems, implying that resolution cannot be improved solely by adding pupil-plane filters to an instrument. However, pupil filters can improve signal-to-noise performance and modify transfer-function zero crossing positions, as demonstrated through a confocal fluorescence example.

OCIS codes: (100.6640) Superresolution; (110.1220) Apertures; (110.4850) Optical Transfer Functions; (180.1790) Confocal Microscopy; (180.2520) Fluorescence Microscopy

References and links

1. C.J.R. Sheppard and Z.S. Hegedus, "Axial behavior of pupil-plane filters," J. Opt. Soc. Am. A **5**, 643-647 (1988).
2. C.J.R. Sheppard, "Leaky annular pupils for improved axial imaging," Optik **99**, 32-34 (1995).
3. S. Grill and E.H.K. Stelzer, "Method to calculate lateral and axial gain factors of optical setups with a large solid angle," J. Opt. Soc. Am. A **16**, 2658-2665 (1999).
4. M. Martínez-Corral, M.T. Caballero, E.H.K. Stelzer and J. Swoger, "Tailoring the axial shape of the point spread function using the Toraldo concept," Opt. Express **10**, 98-103 (2002).
5. D. Mugnai, A. Ranfagni and R. Ruggeri, "Pupils with super-resolution," Phys. Lett. A **311**, 77-81 (2003).
6. M. Martínez-Corral, C. Ibáñez-López and G. Saavedra, "Axial gain resolution in optical sectioning fluorescence microscopy by shaded-ring filters," Opt. Express **11**, 1740-1745 (2003).
7. D.M. de Juana, J.E. Oti, V.F. Canales and M.P. Cagigal, "Transverse or axial superresolution in a 4Pi-confocal microscope by phase-only filters," J. Opt. Soc. Am. A **20**, 2172-2178 (2003).
8. W. Denk, J.H. Strickler and W.W. Webb, "Two-photon laser scanning fluorescence microscopy," Science **248**, 73-76 (1990).
9. S. Hell and E.H.K. Stelzer, "Properties of a 4Pi confocal fluorescence microscope," J. Opt. Soc. Am. A **9**, 2159-2166 (1992).
10. C.W. McCutchen, "Generalized aperture and the three-dimensional diffraction image," J. Opt. Soc. Am. **54**, 240-244 (1964).
11. C.J.R. Sheppard, M. Gu, Y. Kawata and S. Kawata, "Three-dimensional transfer functions for high-aperture systems," J. Opt. Soc. Am. A **11**, 593-598 (1994).
12. M. Gu and C.J.R. Sheppard, "Three-dimensional transfer functions in 4Pi confocal microscopes," J. Opt. Soc. Am. A **11**, 1619-1627 (1994).

#4402 - $15.00 US Received 17 May 2004; revised 13 August 2004; accepted 17 August 2004

13. C.W. McCutchen, "Generalized aperture and the three-dimensional diffraction image: erratum," J. Opt. Soc. Am. A **19**, 1721 (2002).
14. M.R. Arnison and C.J.R. Sheppard, "A 3D vectorial optics transfer function suitable for arbitrary pupil functions," Opt. Commun. **211**, 53-63 (2002).
15. A. Schönle and S.W. Hell, "Calculation of vectorial three-dimensional transfer functions in large-angle focusing systems," J. Opt. Soc. Am. A **19**, 2121-2126 (2002).
16. C.J.R. Sheppard, "The spatial frequency cut-off in three-dimensional imaging," Optik **72**, 131-133 (1986).
17. C.J.R. Sheppard, "The spatial frequency cut-off in three-dimensional imaging II," Optik **74**, 128-129 (1986).
18. B. Richards and E. Wolf, "Electromagnetic diffraction in optical systems II: Structure of the image field in an aplanatic system," Proc. Roy. Soc. A (London) **253**, 358-379 (1959).
19. M. Nagorni and S.W. Hell, "Coherent use of opposing lenses for axial resolution increase in fluorescence microscopy. I. Comparative study of concepts," J. Opt. Soc. Am. A **18**, 36-48 (2001).
20. G. Toraldo di Francia, "Nuovo pupille superresolventi," Atti Fond. Giorgio **7**, 366-372 (1952).
21. T.A. Klar, E. Engel and S.W. Hell, "Breaking Abbe's diffraction resolution limit in fluorescence microscopy with stimulated emission depletion beams of various shapes," Phys. Rev. E **64**, 066613 (2001).
22. R. Heintzmann, T.M. Jovin and C. Cremer, "Saturated patterned excitation microscopy — a concept for optical resolution improvement," J. Opt. Soc. Am. A **19**, 1599-1609 (2002).
23. M. Gu and C.J.R. Sheppard, "Confocal fluorescent microscopy with a finite-sized circular detector," J. Opt. Soc. Am. A **9**, 151-153 (1992).

1. Introduction

Point spread function (PSF) engineering using pupil-filters is currently an active area of research [1-7]. This paper is written to call attention to the fact that the use of pupil filters alone in PSF engineering cannot increase the fundamental achievable resolution for a large class of linear, shift-invariant, far-field optical instruments. The class of optical instruments encompassed includes coherent or incoherent widefield imaging, confocal transmission, reflection or fluorescence imaging, two-photon fluorescence microscopy [8] and 4Pi fluorescence microscopy [9]. A full three-dimensional, vectorial, frequency-domain analysis is used to show the addition of pupil-plane filters will not improve the resolution, as no additional frequency-domain components of the object are passed by the instrument. However, other benefits are possible from pupil filters — a confocal fluorescence example is used to demonstrate benefits in terms of signal-to-noise ratio and imaging with a finite-sized confocal pinhole.

2. Transfer function analysis

This section uses a construction first presented by McCutchen [10] to show that a true resolution increase cannot be achieved through the use of pupil-plane filters. McCutchen's result has also been used and generalized by a number of other authors, e.g. [11-17].

In a three-dimensional, linear, shift-invariant system, the object $o(\mathbf{r})$ ($\mathbf{r}$ is the spatial vector (x,y,z)) can be related to the system output $d(\mathbf{r})$ through a convolution with the point spread function $h(\mathbf{r})$ or through a Fourier domain multiplication with a transfer function.

$$d(\mathbf{r}) = o(\mathbf{r}) * h(\mathbf{r}) \quad \Leftrightarrow \quad D(\mathbf{k}) = H(\mathbf{k})O(\mathbf{k}) \tag{1}$$

Here capitalization represents the Fourier transform and $\mathbf{k}$ is the wavenumber vector (k_x,k_y,k_z). The support of the transfer function $H(\mathbf{k})$ (i.e. the set of $\mathbf{k}$ values for which $H(\mathbf{k})$ is non-zero) has a very strong relationship to the achievable resolution of the system, as it determines which spatial frequencies in the object are passed.

In a far-field imaging system, the form of the point spread function will be intimately tied to the imaging properties of the lens(es) used. A method of calculating the three-dimensional, vectorial distribution of a large-aperture lens' diffraction pattern in the vicinity of the focal point is given in [18]. This distribution, known as the amplitude PSF, can then be used to construct the overall PSF $h(\mathbf{r})$ and the corresponding transfer function can be calculated by taking the Fourier

#4402 - $15.00 US Received 17 May 2004; revised 13 August 2004; accepted 17 August 2004

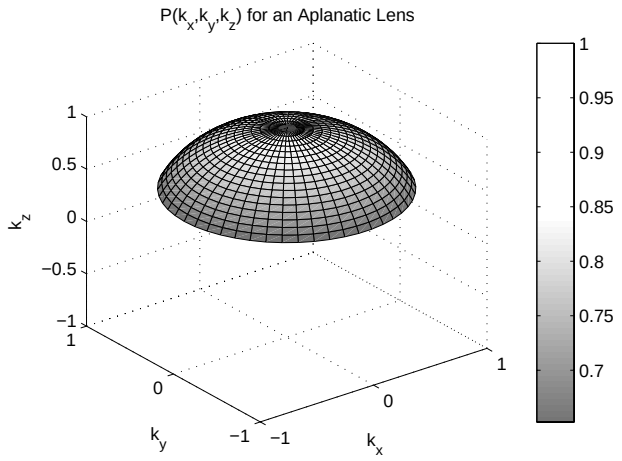

Fig. 1. Graphical representation of the three-dimensional Fourier transform of the amplitude PSF of an aplanatic lens. The maximum collection angle for this plot is 65^o.

transform (see [19] for examples). The transfer function can also be calculated directly. The Fourier domain representation of the scalar amplitude PSF is given in [10]. This representation can then be used to build transfer functions for various instruments entirely in the Fourier domain [11, 12]. More recently, these results have been extended to vectorial optics [13-15].

Constructing the transfer function directly allows insight to be gained about its properties. Of particular interest is the region over which the transfer function is non-zero — i.e. its support. The support of the transfer function determines which spatial frequencies of the object are passed by the system and hence which may be recovered in the image. This ultimately determines the maximum achievable resolution. Examples of this type of analysis can be seen in [16, 17].

Let the Fourier transform of the amplitude PSF of a lens be given by $P(\mathbf{k})$. This function is non-zero only on a very specific region. Let the x and y coordinates be in the plane of focus (the lateral dimension), z along the optic axis (the axial dimension) and the nominal focus at $\mathbf{r} = \mathbf{0}$. In the frequency domain let $\theta = \tan^{-1}(\sqrt{k_x^2 + k_y^2}/k_z)$ — this is the angle from the k_z axis. The support of $P(\mathbf{k})$ is given as follows.

$$\begin{aligned} S_P &= \{\mathbf{k} : P(\mathbf{k}) \neq 0\} \\ &= \left\{\mathbf{k} : |\mathbf{k}| = \frac{2\pi n}{\lambda}, \theta \leq \sin^{-1}\left(\frac{NA}{n}\right)\right\} \end{aligned} \tag{2}$$

In the above equation n is the refractive index of the medium, λ is the free-space wavelength and NA is the lens' numerical aperture. The constraint on the magnitude of $\mathbf{k}$ shows that the amplitude PSF is constructed only from plane waves with a spatial frequency corresponding to the wavelength used. The second constraint (on θ) restricts the directions of propagation that can be used. Thus S_P is a spherical cap where the radius of the sphere depends on the wavelength used and the angular extent depends on the maximum collection angle of the lens. A graphical representation of this is shown in Fig. 1.

The function $P(\mathbf{k})$ is a delta sheet that is non-zero only on S_P and weighted by some apodization function $A(\mathbf{k})$ (the apodization function is scalar if a scalar analysis is used and a three-dimensional vector function if vector optics are used). For an aplanatic lens, conservation of energy leads to an apodization function of the form $\sqrt{\cos(\theta)}$ [18], as shown in Fig. 1. The

#4402 - $15.00 US Received 17 May 2004; revised 13 August 2004; accepted 17 August 2004

apodization function can be modified to account for aberrations or defocus, in which case it may be necessary to use a complex $A(\mathbf{k})$. The effect of pupil-plane filters is to change the apodization function. The pupil-filter effect may consist of a change in transmittance, in which case the magnitude of $A(\mathbf{k})$ will be affected and/or a change in the phase of $A(\mathbf{k})$. An example of changing the transmittance is considered later in this paper. The Toraldo concept [20] is an example of a technique that only modifies the phase and has recently been the subject of further investigation [4, 5].

The amplitude PSF is represented in the Fourier domain by $P(\mathbf{k})$ and this is the transfer function for widefield coherent imaging. The PSF for widefield incoherent imaging is simply the intensity of the amplitude PSF. Basic Fourier transform properties mean that the widefield incoherent transfer function is the autocorrelation of $P(\mathbf{k})$. The support of the transfer function is therefore given by the range of offsets over which two $P(\mathbf{k})$ functions will overlap. Similar arguments can be made for confocal imaging systems [11]. For the incoherent confocal case the PSF is the product of two widefield incoherent PSFs and thus the transfer function is the convolution of two autocorrelations of $P(\mathbf{k})$ functions. The transfer function of a 4Pi system can also be constructed directly in the Fourier domain [12]. In this case the result is the convolution of two autocorrelations of $[P(\mathbf{k})+P(-\mathbf{k})]$ functions. Changing the apodization function(s) won't change the support of these transfer functions. The resolution of these systems increases from widefield to confocal to 4Pi due to differences in the optical setup, which result in transfer function constructions with increased support. The addition of pupil-plane filters changes only the magnitude and/or phase of the apodization function(s) and not the construction methods. Since the support depends only on the construction method and the support of the $P(\mathbf{k})$ functions, the pupil-filters do not increase the transfer function support.

This type of Fourier-domain transfer function construction can be carried out for coherent or incoherent widefield imaging, confocal transmission, reflection or fluorescence imaging, two-photon fluorescence microscopy and 4Pi fluorescence microscopy. Thus a change in the apodization function(s) will not change the support of any of these transfer functions. This implies that the addition of pupil filters will not change the maximum achievable resolution. More generally, basic Fourier transform properties can be used to show that any PSF constructed by sum, multiplication, intensity, rotation, convolution and/or shift (defocus) operations on a set of amplitude PSFs will have a transfer-function support that is unchanged by the addition of pupil-plane filters. This is because the support of the overall transfer function depends only upon the support of the constituent $P(\mathbf{k})$ functions and not the values of the apodization functions. Physically, the range of spatial frequencies passed by the system is influenced only by the spatial frequencies collected by the lenses and not their relative strengths. An important caveat to this result is that within the calculated support the transfer function may have zero crossings. In this case pupil-plane filters may be able to shift the zero crossings and thus allow previously unobservable components of the object to be imaged. An example of this effect is provided later in the paper. Several modern instruments rely on non-linear optical phenomena [21, 22] and will not be included in the class of instruments to which this paper is applicable.

3. Performance in the presence of noise

While pupil-plane filters cannot increase the transfer function support, they do have utility in boosting the signal-to-noise ratio (SNR). This point and the fact that the transfer function support cannot be enlarged will be demonstrated here with a confocal fluorescence example from [6].

The point spread function of a confocal fluorescence microscope depends on the two amplitude PSFs present in the system — the excitation amplitude PSF $p_{ex}(\mathbf{r})$ and the detection

#4402 - $15.00 US Received 17 May 2004; revised 13 August 2004; accepted 17 August 2004

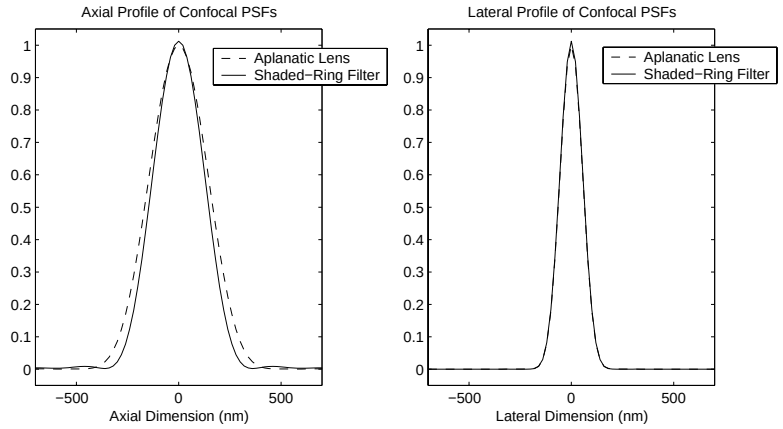

Fig. 2. Lateral and axial profiles along the axes for the confocal fluorescence point spread functions. One system is aplanatic while the other uses a shaded-ring pupil filter for the excitation. Note that the lateral profiles are too similar to distinguish.

amplitude PSF $p_{det}(\mathbf{r})$. The overall PSF can be written as follows.

$$h(\mathbf{r}) = |p_{ex}(-\mathbf{r})|^2 |p_{det}(-\mathbf{r})|^2 \tag{3}$$

In the Fourier domain Eq. 3 becomes the following.

$$H(\mathbf{k}) = [P_{ex}(-\mathbf{k}) \star P_{ex}(-\mathbf{k})] * [P_{det}(-\mathbf{k}) \star P_{det}(-\mathbf{k})] \tag{4}$$

Here $\star$ represents the autocorrelation operation and $*$ represents convolution.

The PSF for a confocal fluorescence microscope was calculated using the same method as [19] (which is based on the vector optics results presented in [18]). The physical parameters of the system were chosen to match those used in the shaded-ring pupil filter example of Fig. 2 in [6] — specifically, the excitation wavelength is 350 nm, the detection wavelength is 440 nm and the maximum collection angle is 64.5^o (this corresponds to a numerical aperture of 1.2 in water). The PSF for the shaded-ring system was also calculated. Lateral ($\sqrt{x^2+y^2}$) and axial (z) sections (through the origin) of these two point spread functions are shown in Fig. 2. The images have been scaled so that the excitation powers are equal which means that equal photobleaching would occur using either system.

In Fig. 2 it can be seen that the pupil-plane filter has changed the shape of the PSF. As claimed in [6], the effect has been to reduce the axial extent of the point spread function. This axial narrowing of the shaded-ring system's PSF suggests an improved axial resolution. However, when the transfer functions are calculated it becomes apparent that the Fourier domain support has not changed. Lateral and axial sections of the transfer functions on a semilogarithmic scale are plotted in Fig. 3. They were calculated by taking the Fourier transform of the PSFs of Fig. 2 and normalizing so that the maximum value of the aplanatic-lens transfer function was 1. The maximum extents of these transfer functions were calculated theoretically [23] to be 3.88 μm $^{-1}$ axially and 12.3 μm^{-1} laterally. The cutoff frequencies for both systems are equal and agree with the theoretical figures (the low values outside the theoretical support are below calculation precision).

In Fig. 3 it can be seen that axial frequencies near the cutoff are passed more strongly by the shaded-ring-filter system (the maximum ratio between the two transfer functions is approximately 3.5). This effect could be synthesized in the aplanatic data by applying a linear

#4402 - $15.00 US Received 17 May 2004; revised 13 August 2004; accepted 17 August 2004

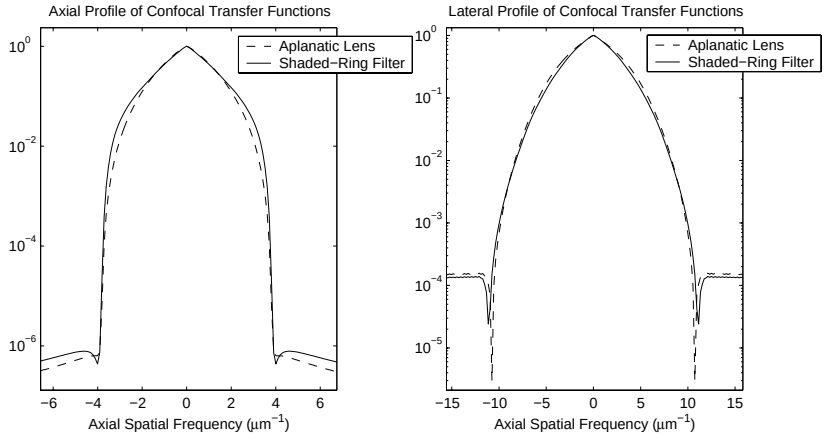

Fig. 3. Lateral and axial profiles along the axes for the confocal fluorescence transfer functions. One system is aplanatic while the other uses a shaded-ring pupil filter for the excitation.

post-processing filter to boost the high axial frequencies. Thus the effect of the pupil filters can be regarded as a physical implementation of an edge-enhancing high-boost filter and not true superresolution. The noise level in the two systems will be comparable as the overall signal strength is largely determined by the low-frequency values of the transfer functions, which are similar. Since the high-frequency information is more strongly passed in the pupil-filter system, the SNR will be improved at these frequencies. Thus for the high axial frequencies, the SNR is improved by the application of this shaded-ring pupil filter. It worth noting that the linear processing operation performed by the inclusion of pupil-plane filters does not require the collection of a complete data set, as computational Fourier-domain processing methods do. This physical implementation of linear processing may also have advantages over computational methods in coherent systems where phase information can be lost at detection.

4. Detector aperture effects and modifying zero-crossing positions

In this section it is noted that there are scenarios in which a transfer function may have zero crossings within its calculated support. In these cases pupil-plane filters may be used to shift the zero crossings and thus, ideally, change the spatial frequency components of the object that can be observed in the image. This is demonstrated for completeness and is not meant to suggest that pupil filters are a practical way of addressing the problem of zero-crossings in a transfer function.

In the previous confocal example, the transfer function was strictly positive over the whole support. When the effects of aberrations or a finite-sized detection pinhole are considered, this positivity property is not necessarily retained [23]. The effect of the pinhole is to multiply the detection component of the transfer function by the Fourier transform of the pinhole. The Fourier transform of the circular pinhole used here does have negative values. When the resulting detection component of the transfer function is convolved with the excitation component (see Eq. 4) the result may also be negative or zero for particular **k** values. In [23] it is shown that for larger pinholes the transfer function will become negative in certain areas and will thus have zero-crossings within the support. At these zero crossings the corresponding spatial frequency is unobservable and in the vicinity of the zero crossings the SNR is very poor. Using a pupil filter in the excitation will give different values to the excitation component of the trans-

#4402 - $15.00 US Received 17 May 2004; revised 13 August 2004; accepted 17 August 2004

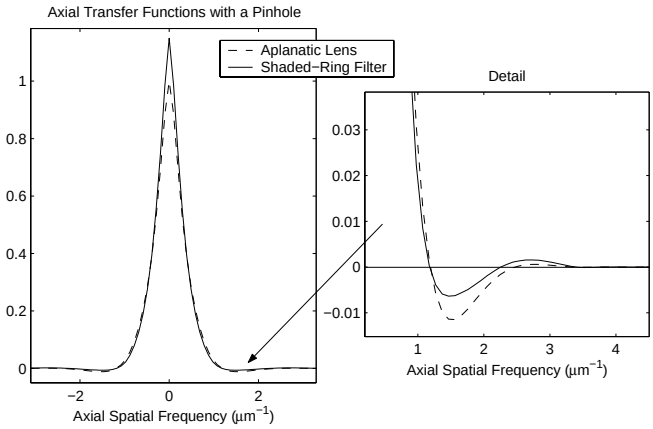

Fig. 4. Axial profiles along the z axis for the confocal fluorescence transfer functions when a large detector pinhole is used. One system is aplanatic while the other uses a shaded-ring pupil filter for the excitation.

fer function, so that when convolved with the detection component the zero crossings may no longer occur in the same position.

In Fig. 4 the axial profile of the transfer functions are shown when a large circular detector pinhole of radius 600 nm (when projected into object coordinates) is added to the previous example. The transfer functions are again normalized so that the aplanatic transfer function has a maximum value of 1. The plots are now on a linear scale and a detail of the zero crossings is shown. In Fig. 4 it can be seen that the excitation pupil filter has had the effect of moving the zero crossings on the axial axis (the lateral changes are not significant). This means that there are spatial frequency components of the object that are visible in the pupil-filter data but cannot be seen in the aplanatic data (and vice versa). It should be noted that a similar zero-crossing shifting could be achieved by simply using a pinhole of a different size.

5. Conclusions

For a considerable class of optical instruments the use of pupil-plane filters cannot increase the support of the system's transfer function, which implies that they offer no fundamental increase in achievable resolution despite suggestive spatial domain results. The reasoning behind this result is evident in the derivations contained in the microscopy transfer-function literature cited here. Benefits of pupil filters were shown by example. Specifically, pupil filters can be used to improve the imaging of high spatial frequencies (which correspond to fine detail) in the presence of noise. They may also be used to shift the zero crossings in a transfer function and thus change the unobservable spatial frequencies within the transfer function support. Pupil-filter PSF engineering also has many practical applications not discussed here (e.g. increasing the depth of focus in two-dimensional microscopy).

Acknowledgments

The authors would like to thank Dr. Rainer Heintzmann, Dr. Lukas Novotny and the anonymous reviewers for their insightful comments and suggestions. This work was partially supported by the NIH under grant NIH R01 EB756-01, by the NSF under grant NSF DBI 0138425 and by the Engineering Research Centers Program of the National Science Foundation under award number EEC-9986821.